iScience

CellPress
OPEN ACCESS

Article

Supplementing a specific synbiotic suppressed the incidence of AOM/DSS-induced colorectal cancer in mice

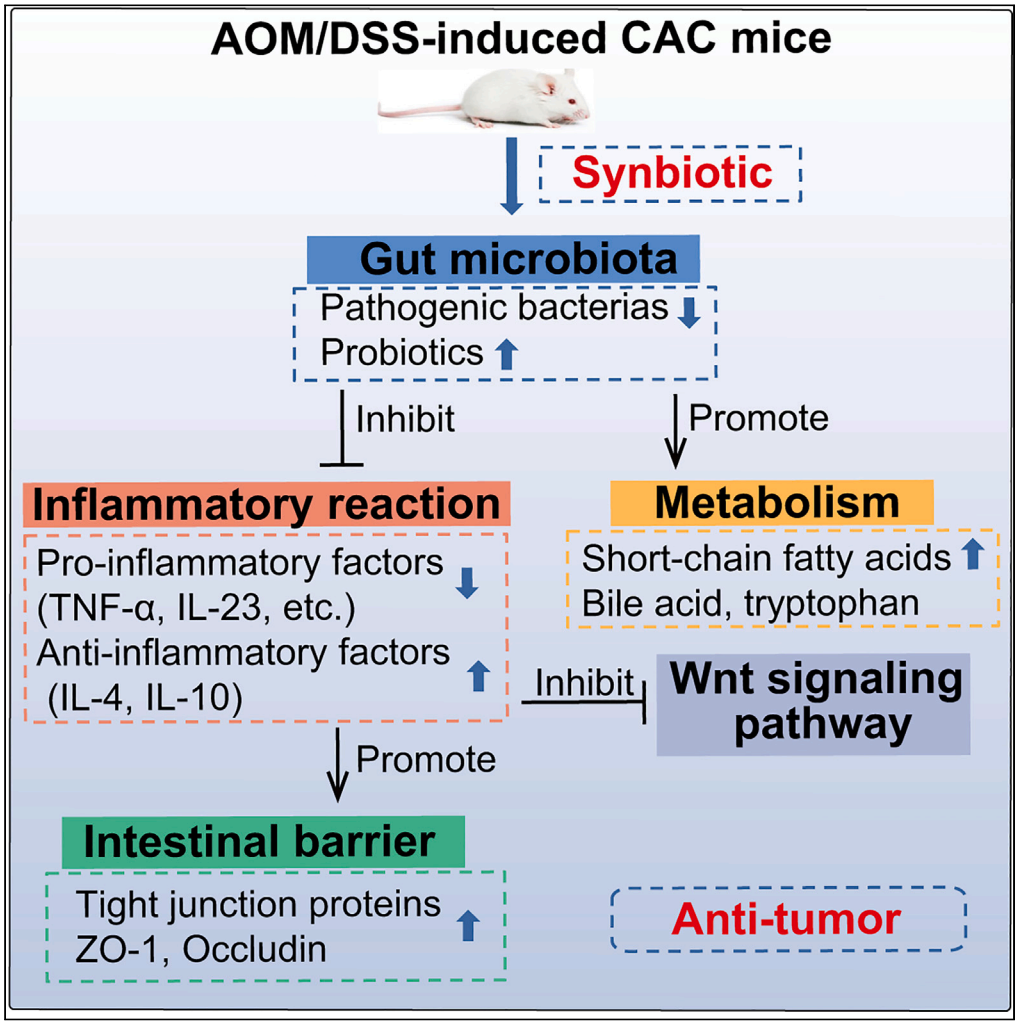

Huixia Wu, Zhengchun Wu, Yilan Qiu, ..., Jian Chen, Yiliang Zeng, Rushi Liu

liurushi@hunnu.edu.cn

Highlights

The synbiotic can alleviate colon inflammation and intestinal mucosal barrier damage

The synbiotic can change the microbiota and the metabolome in CAC mice gut

The synbiotic can inhibit the activation of the Wnt/β-catenin signaling pathway

Wu et al., iScience 26, 106979
June 16, 2023
https://doi.org/10.1016/j.isci.2023.106979

iScience

CellPress
OPEN ACCESS

Article

Supplementing a specific synbiotic suppressed the incidence of AOM/DSS-induced colorectal cancer in mice

Huixia Wu,[1,7] Zhengchun Wu,[2,7] Yilan Qiu,[3,6] Fangjian Zhao,[4] Minjing Liao,[1] Zhihong Zhong,[1] Jian Chen,[4] Yiliang Zeng,[5] and Rushi Liu[1,8,*]

SUMMARY

In this study, we evaluated the effect of a specific synbiotic on CAC (AOM/DSS-induced colitis-associated cancer). We confirmed that the synbiotic intervention was able to protect the intestinal barrier and inhibit CAC occurrence via upregulating tight junction proteins and anti-inflammatory cytokines, and downregulating pro-inflammatory cytokines. Moreover, the synbiotic significantly improved the disorder of the colonic microbiota of CAC mice, promoted the formation of SCFAs and the production of secondary bile acids, and alleviated the accumulation of primary bile acids in the CAC mice. Meanwhile, the synbiotic could significantly inhibit the abnormal activation of the intestinal Wnt/β-catenin signaling pathway significantly related to IL-23. In a word, the synbiotic can inhibit the occurrence and development of colorectal tumors and it may be a functional food to prevent inflammation-related colon tumors, and the research also provided a theoretical basis for improving the intestinal microecological environment through diet therapy.

INTRODUCTION

Colorectal cancer (CRC) is the second leading cause of cancer death worldwide, and its incidence is gradually increasing among people under the age of 50 years.[1,2] CRC is an intestinal epithelial heterogeneous disease with mutation accumulation and immune imbalance.[3] Although the true culprit of CRC remains be clarified, a large amount of evidence show that the incidence of CRC partly owes to inflammation of inflammatory bowel disease (IBD).[4] IBD can evolve into CRC, which can be replicated with AOM (azoxymethane) and DSS (dextran sulfate sodium) induction in mice. Anti-inflammatory drugs can effectively suppress the progression of IBD to CRC,[5,6] but these drugs are not meant for long-term use due to their serious side effects.[7] Therefore, it is urgent to develop a more effective and safer strategy to cure IBD and prevent IBD from progressing to CRC.

Synbiotics, mainly composed of prebiotics and probiotics, can regulate the intestinal microbiota as a dietary intervention method. Probiotics, a kind of living microorganisms, are beneficial to health on the host, including *Bifidobacterium*, *Lactobacillus*, *Streptococcus*, and so on. Prebiotics, an indigestible dietary fiber, can selectively stimulate the growth and activity of probiotics in the colon, thereby functioning a beneficial effect on the host,[8] such as inulin, fructooligosaccharide (FOS), galactooligosaccharides, etc.[9] A previous study revealed that supplementation of FOS can significantly increase the abundance of *Bifidobacterium* in the intestinal microbiota.[10] Over long evolution, the mammalian colon coexists peacefully with diverse gut microbiota, which promotes the mutual benefit between the host and the gut microbial community.[11] It has been reported that *Lacticaseibacillus paracasei* can relieve the symptoms of colitis in mice.[12] A previous study found that β-galactosidase secreted by *Streptococcus thermophilus* plays an antitumor role and can be used as a new strategy to prevent colorectal cancer in mice.[13] Similarly, prophylactic supplementation of synbiotics can improve the composition of intestinal microbiota and intestinal microenvironment, increase the abundance of *bifidobacteria* and *Lactobacillus*, and increase the concentration of total organic acids (especially acetic acid).[14] Furthermore, it has been revealed that synbiotics (*Lacticaseibacillus rhamnosus GG* strain + dietary fiber) can significantly inhibit the proliferation of colorectal cancer cells compared with probiotic or prebiotic treatment alone.[15] Additionally, our previous research also confirmed that the regulation of intestinal microbiota by FOS or a specific synbiotic

[1]Department of Medical Laboratory, School of Medicine, Hunan Normal University, Changsha 410013, China

[2]Department of Hepatobiliary and Intestinal Surgery, Hunan Cancer Hospital and the Affiliated Cancer Hospital of Xiangya School of Medicine, Central South University, Changsha 410013, China

[3]School of Life Science, Hunan Normal University, Changsha 410018, China

[4]Medical Laboratory, The First Affiliated Hospital of Hunan Normal University, Changsha 410018, China

[5]Shaoshan Changbaitong Biological Technology Co., Ltd., Shaoshan 411100, China

[6]Changsha Tianan Biotechnology Co., Ltd., Changsha 410018, China

[7]These authors contributed equally

[8]Lead contact

*Correspondence: liurushi@hunnu.edu.cn

https://doi.org/10.1016/j.isci.2023.106979

(composed of FOS and 8 probiotic strains) supplement can reduce the inflammatory potential of colonization symbionts, so as to prevent the damage of intestinal barrier in mice with DSS-induced acute colitis and induce the regulation of immune response.[16] Based on our previous study, we speculated that the synbiotic could inhibit the CRC tumorigenesis. Thus, we investigated the role of the synbiotic in CRC tumorigenesis and its potential mechanism in this study to provide new insight into CRC prevention and treatment.

RESULTS

The synbiotic intervention significantly improves the pathological phenotype of CAC mice

The AOM/DSS-induced colitis-associated cancer (CAC) model was used to observe the preventive effect of the specific synbiotic on the carcinogenesis of colorectal cancer (Figure 1A). The weight of mice decreased significantly under DSS induction, while the weight of mice recovered gradually under withdrawal of DSS. The intervention of the synbiotic could obviously alleviate the weight loss of mice (Figure 1B). Compared with the normal control group mice, the colon length of AOM/DSS group mice was significantly shortened, and tumors occurred in the AOM/DSS group mice. While under the intervention of the synbiotic, the colon length of AOM/DSS group mice was restored, and the tumor number and volume decreased significantly, and the proportion of tumors with a diameter over 2 mm was significantly reduced (Figures 1C–1F). HE staining showed that the colon of the control group mice presented intact colonic epithelium, intestinal glands, mesenchyme, and submucosa. While the colon of the AOM/DSS group mice exhibited surface epithelial erosion, crypt destruction, mucosal muscle destruction, submucosal edema, inflammatory cell infiltration, intraepithelial neoplasia, and cancer cells. However, under the synbiotic treatment, the structure of intestinal mucosal crypts was relatively well maintained (Figure 1G).

The synbiotic intervention effectively restores colonic mucosal barrier damage in CAC mice

It is known that tight junctions play a vital role in maintaining the integrity of cells, and their loss can accelerate the pathogenesis and development of various gastrointestinal disease (such as IBD, irritable bowel syndrome, and even colorectal cancer).[3,17] Therefore, we further investigated the effect of the synbiotic on the expression of tight junction proteins including zonula occludens 1 (ZO-1) and occludin. Compared with the control group mice, the expression of ZO-1 and occludin in the AOM/DSS group mice was significantly downregulated. However, under the intervention of the synbiotic, the expression of ZO-1 and occludin was significantly restored (Figures 2A and 2B). This result indicated that prophylactic supplementation of the synbiotic can protect the intestinal epithelial barrier by regulating tight junction proteins in CAC mice induced by AOM/DSS.

The synbiotic intervention suppresses the inflammation in CAC mice

Inflammatory molecules are involved in various processes of colitis-related colon cancer. Thus, the expression typical pro-inflammatory and anti-inflammatory cytokines in colon tissue were tested in this study. Compared with normal control mice, a variety of pro-inflammatory factors' (*Il1β*, *Il12b*, *Il17A*, *Tnf-α*, *Il-23*, and *COX-2*) expression increased significantly in mRNA level. However, under the intervention of the synbiotic, the mRNA expression of these inflammatory factors decreased gradually. In contrast, the mRNA expression of the anti-inflammatory cytokines *Il4* and *Il10* in the colon tissue of AOM/DSS group was significantly reduced, while the synbiotic intervention upregulated significantly the expression of *Il4* mRNA and *Il10* mRNA (Figure 2C). Furthermore, western blotting further verified the expression of TNF-α and IL-23 in protein level (Figure 2D). These results indicated that the synbiotic used in this study can effectively protect the intestinal barrier by inhibiting colonic inflammatory response.

The synbiotic intervention adjust the structure of intestinal microbial community

To evaluate the effect of the synbiotic on the gut microbiota in CAC mice, the colon contents of mice were collected and were then tested via 16S rDNA microbiota sequencing. The results showed that the number of OTUs in AOM/DSS group mice (1583) was significantly reduced compared with the control group mice (2112). Under the intervention of the synbiotic, the number of OTUs of AOM/DSS_Synbiotic mice significantly recovered to 1803 (Figure S1). Alpha diversity analysis is a comprehensive index to assess species richness (Chao1) and diversity (Shannon and Simpson index). The colonic bacterial population of the AOM/DSS group mice significantly reduced compared with the control group mice. Under the synbiotic intervention, the relative abundance of intestinal microbes significantly increased, and the diversity showed an increasing trend which was not significantly different (Figure 3A). However, principal component analysis (principal co-ordinates analysis) showed that among the control group, AOM/DSS group,

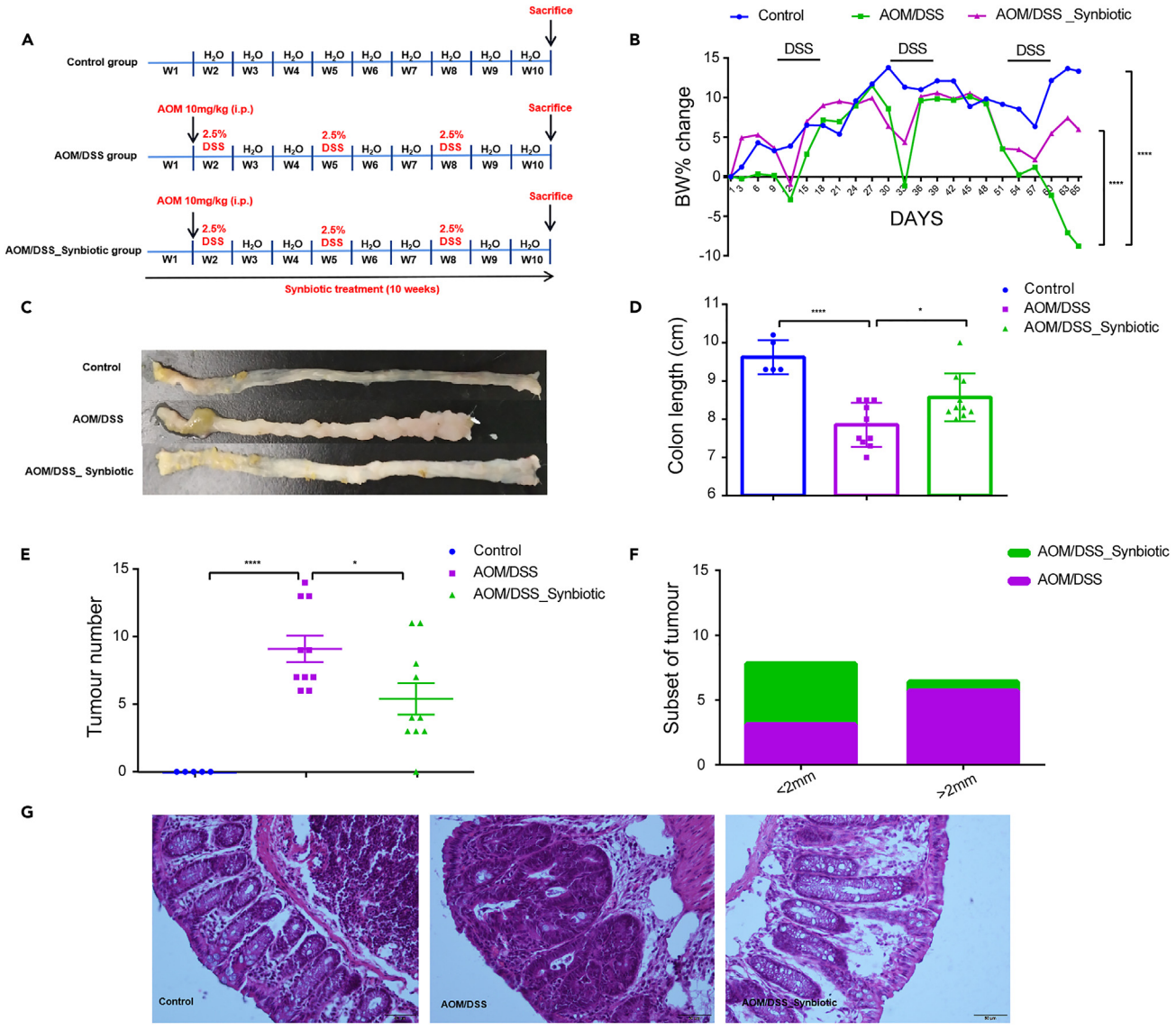

Figure 1. The occurrence and development of tumors in AOM/DSS mice and AOM/DSS_Synbiotic

(A) The establishment of AOM/DSS-induced CAC model and the experimental protocol of the synbiotic intervention. The mice in the model group were injected with AOM (10 mg/kg) intraperitoneally first, and then allowed to drink 2.5% DSS drinking water freely for a week, and then change to sterilized water and drink freely for 2 weeks to recover; take this as a cycle and repeat 3 times. Mice in the intervention group are gavaged with the synbiotic intervention preparations every day.

(B) The average weight change percentage of mice.

(C and D) Comparison of the colon length among different groups.

(E and F) Comparison of tumor number and size among mice.

(G) HE staining of colon tissue (ruler, 50μm). (Statistical analysis of data is expressed by mean ± SEM; *p < 0.05, **p < 0.01, ***p < 0.001, ****p < 0.0001, n = 5–10, Student's t-test.).

and the AOM/DSS_Synbiotic group, the similarities and microbiota structure were significantly different (Figure S2). Therefore, we further investigated the classification spectrum of bacteria at the phylum level (Figure 3B). 19 phyla were detected in all samples, among which *Bacteroidetes* and *Firmicutes* were the most abundant phyla. Compared with the normal control group, the relative abundance of *Firmicutes* significantly reduced, the relative abundance of *Bacteroidetes* increased (Figure S3), and the ratio of *Firmicutes* to *Bacteroidetes* significantly decreased in the AOM/DSS group. However, the synbiotic intervention significantly reversed this trend (Figure 3C). Under the synbiotic intervention, *Burkholderiaceae*,

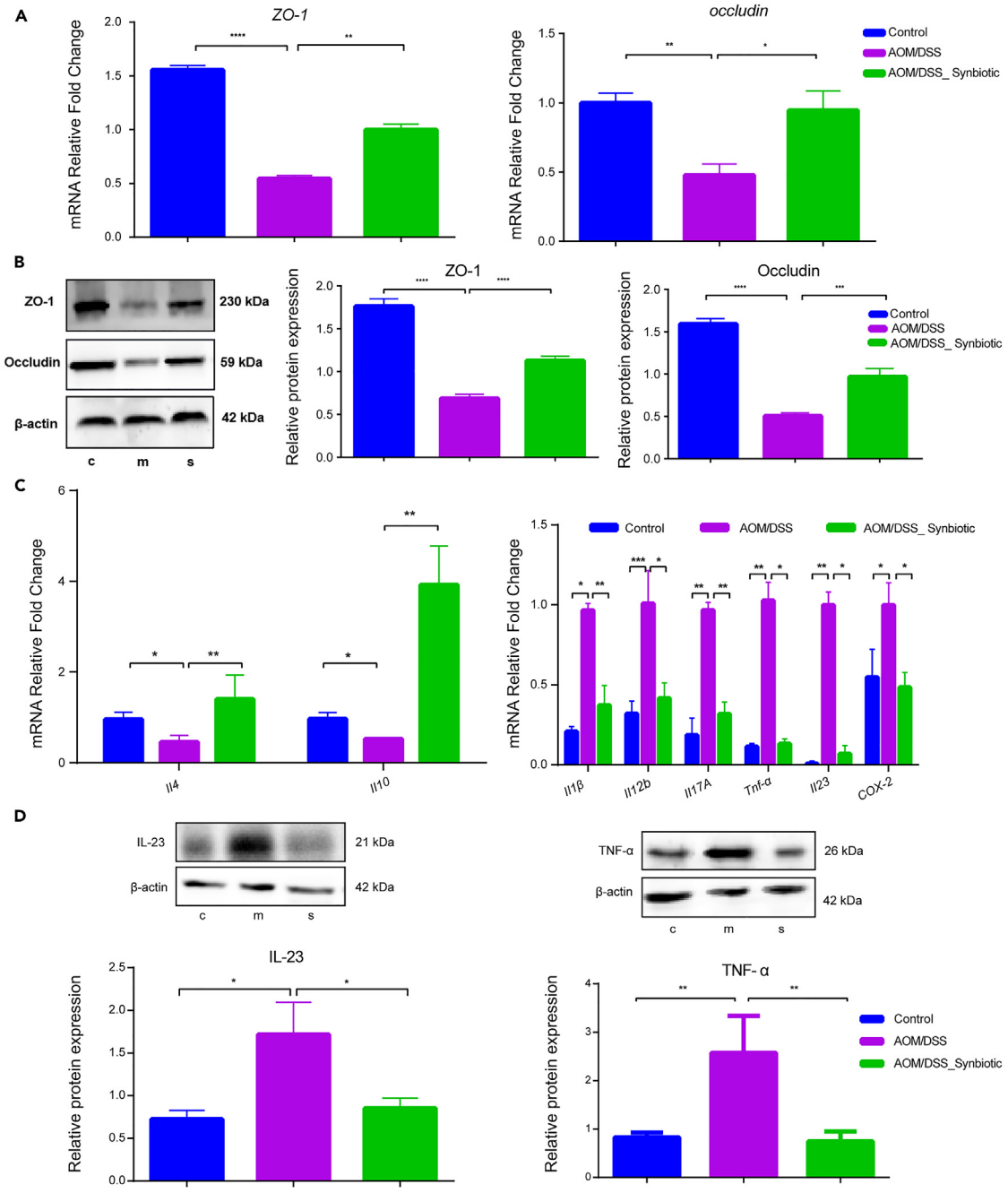

Figure 2. The synbiotic supplementation prevented the loss of epithelium tight junction proteins in AOM/DSS-induced CAC mice

(A) qRT-PCR was used to detect the mRNA expression of *ZO-1* and *occludin* in colon tissues of mice;

(B) Western blotting was used to detect the expression of ZO-1 and occludin in colon tissues of mice;

(C) qRT-PCR was used to detect the mRNA expression of cytokines in colon tissues of mice;

(D) Western blotting was used to detect the expression of TNF-α and IL-23 in colon tissues of mice. (Statistical analysis of data is expressed by mean ± SEM; *p < 0.05, **p < 0.01, ***p < 0.001, ****p < 0.0001, (n = 5–10), Student's t-test.). COX-2, Cyclooxygenase-2; TNF-α, Tumor necrosis factor alpha; ZO-1, Zonula occludens 1.

Peptococcaceae, and *Deferribacteraceae* showed an increasing trend at the family level, while *Pasteurellaceae*, *Streptococcaceae*, *Sphingomonadaceae*, *Pseudomonadaceae*, and *Enterococcaceae* significantly reduced (Figure S4). These results demonstrated that the variation of types of colonic microorganisms occurred under the synbiotic intervention.

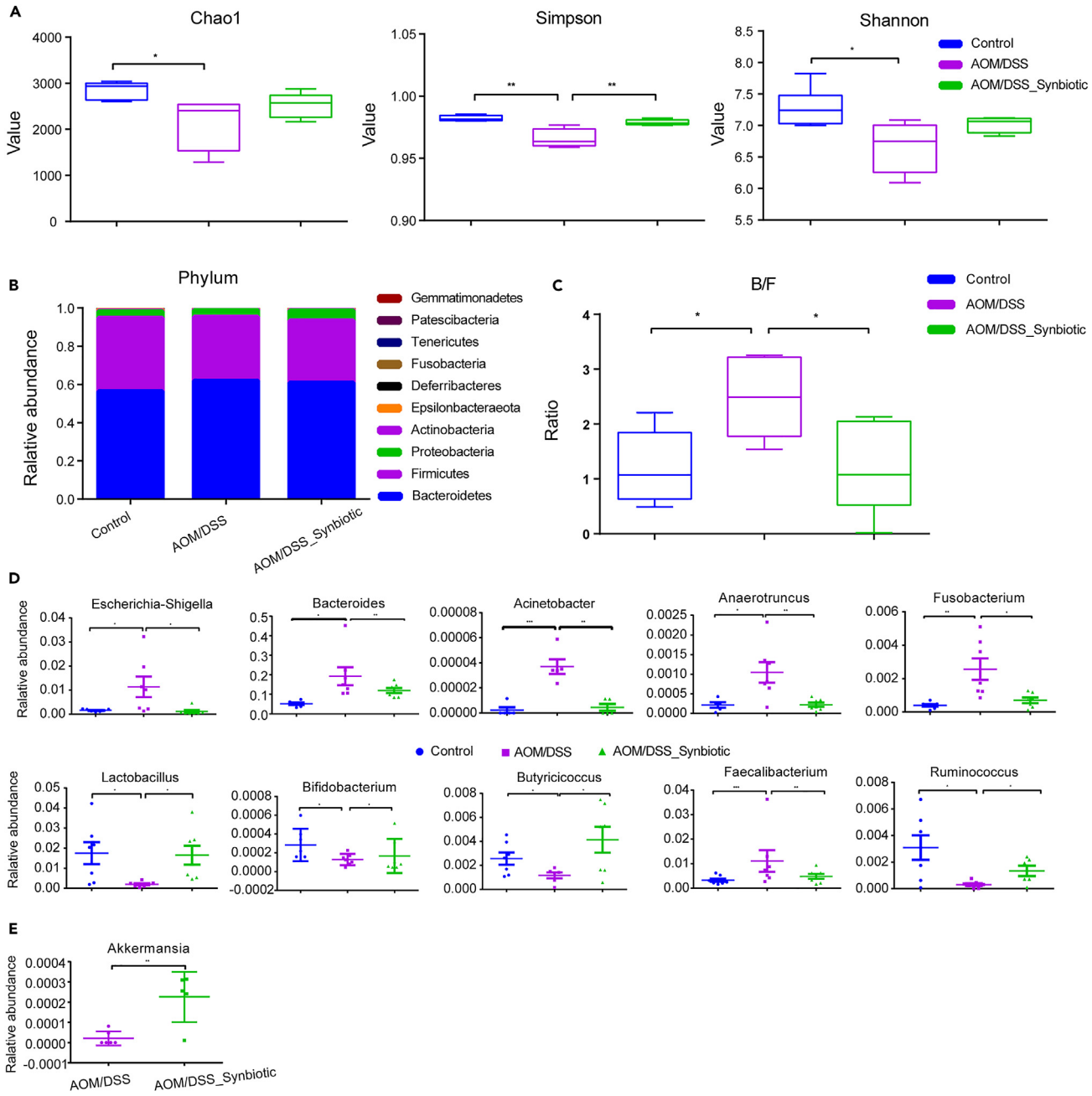

Figure 3. 16S rDNA sequencing tested gut microbes in CAC mice induced by AOM/DSS

(A) α diversity analysis, which are Chao 1 index, Simpson index, Shannon index, respectively.

(B) Statistical analysis of gut microbes at the phylum (L2) level.

(C) Ratio of *Bacteroidetes* to *Firmicutes* in each group.

(D) Comparison of key different species at the genus level in each group.

(E) Statistical analysis of different species *Akk* at the species level. (Data were presented as mean ± SEM; *p < 0.05, **p < 0.01, ***p < 0.001, n = 4–10, Student's t-test.).

Additionally, certain conditional pathogenic bacteria significantly increased in the AOM/DSS group, such as *Escherichia-Shigella*, *Bacteroides_fragilis*, *Acinetobacter*, *Anaerotruncus*, and *Fusobacterium nucleatum*, while the relative abundance of beneficial bacteria remarkably decreased, such as *Lactobacillus*, *Bifidobacterium*, *Ruminococcus Roseburia*, *Butyricicoccus*, *Faecalibacterium*, *Roseburia*, *Subdoligranulu*, and *Clostridium leptum*. Under the synbiotic intervention, the abundance of colonic beneficial bacteria in the

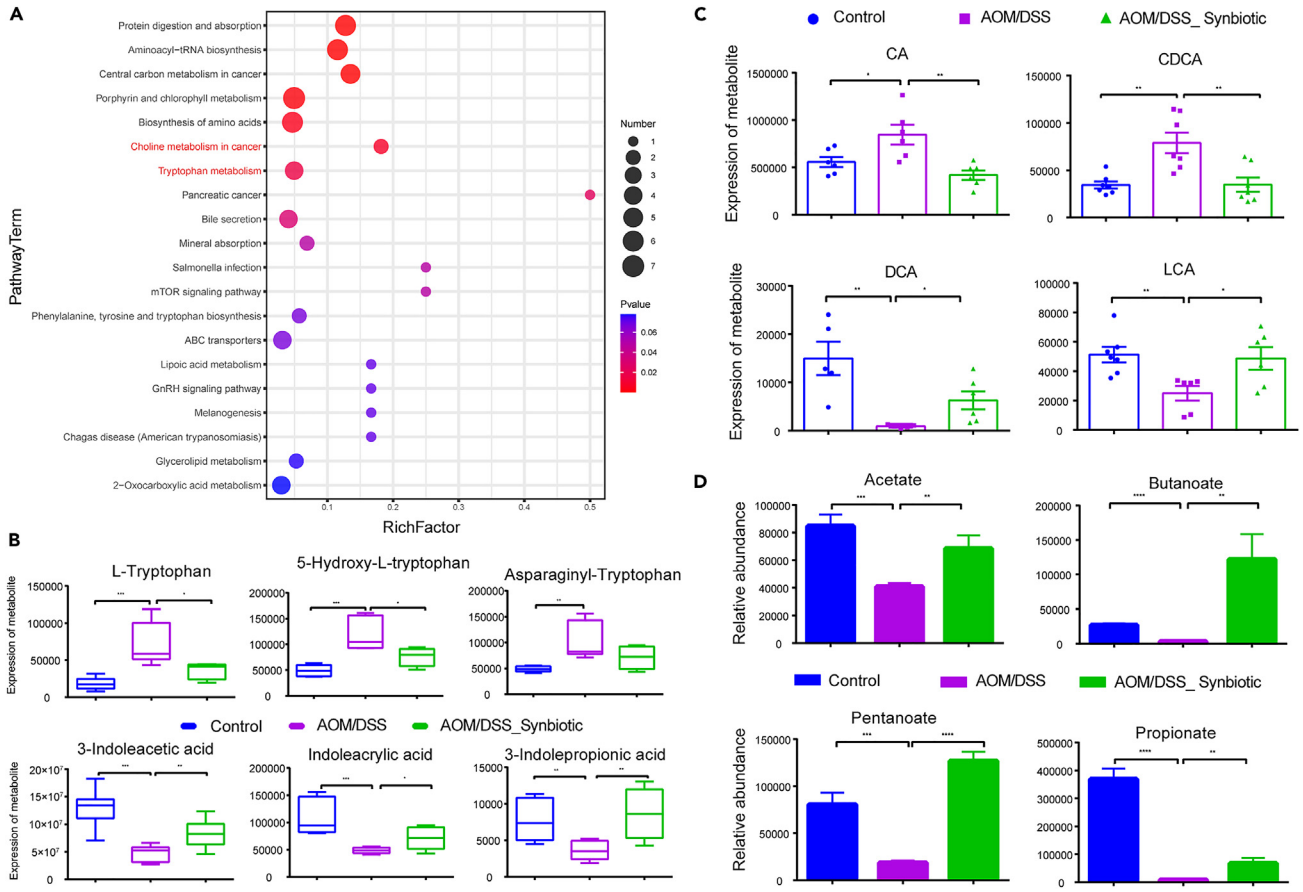

Figure 4. Screening key differential metabolites of mouse colon contents using non-targeted metabolomics methods

(A) According to the significant difference in colon content, the metabolite TOP-20 was used to draw a bubble chart of metabolic pathway enrichment.

(B)Analyzing the levels of tryptophan in colon contents (L-tryptophan, asparaginyl-tryptophan, 5-hydroxy-L-tryptophan) and the levels of tryptophan metabolites (IPA, IAA, and IA).

(C) Statistics of the difference levels of bile acids (CA, CDCA, DCA, and LCA) in the colon contents of each group.

(D) Comparing the intestinal SCFA (acetic acid, propionic acid, butyric acid, and valeric acid) content among different groups. (Data are presented as mean ± SEM; *p < 0.05, **p < 0.01, ***p < 0.001, ****p < 0.0001, n = 5–10, Student's t-test.).

AOM/DSS group could recover to normal levels (Figures S5 and 3D) and *Roseburia*, *Subdoligranulu*, and *C. leptum* (Figure S6) decreased remarkably. With the synbiotic intervention, the abundance of gut beneficial bacteria in the AOM/DSS group mice can restore to normal levels.

Subsequently, we further compared the different bacteria at the species level, and the probiotic *Akkermansia* significantly increased in the mice treated with the synbiotic (Figure 3E). These above results demonstrated that the intervention of the synbiotic can effectively alleviate the disorder of the intestinal microbiota structure during the tumorigenesis of CAC, which further suppress gut inflammation and the oncogenesis and development of CAC.

The synbiotic can regulate the metabolism of tryptophan and bile acid, and promote the production of SCFA by the intestinal microbiota

The influence of gut microbes on the host involves a series of complex interactions between the host-microbe axis. However, small-molecule metabolites are the key to coordinating this interaction.[18,19] Investigating the metabolic alternations caused by gut microbes are contributed to understand the biochemical mechanism of the synbiotic suppressing AOM/DSS-induced CAC tumorigenesis. Therefore, non-targeted metabolomics was performed to analyze the metabolites in the colon contents of mice. Metabolomics results showed that metabolites of colon contents were significantly different among different groups (Figure S7), which involved tryptophan metabolism and bile acid metabolism (Figure 4A). The levels of

L-tryptophan, 5-hydroxy-L-tryptophan, and asparaginyl-tryptophan in the AOM/DSS group significantly increased. The levels of indole acetic acid (IAA), indole propionic acid (IPA), and indole acrylic acid (IA) significantly reduced in the AOM/DSS group (Figure 4B). Compared with the normal control group, primary bile acid including cholic acid and chenodeoxycholic acid significantly accumulated, and the levels of secondary bile acid including deoxycholic acid and lithocholic acid significantly decreased in the AOM/DSS group. The variation of these metabolites was obviously reversed with the intervention of the synbiotic (Figure 4C). Additionally, short-chain fatty acids (SCFA) are produced by intestinal microbiota, especially *Lactobacillus* and *Bifidobacterium*.[20] Under the synbiotic intervention, bacteria producing SCFA significantly increased (Figure 3D), and the content of four SCFAs remarkably increased (Figure 4D). Combined with previous reports,[21] we speculated that the synbiotic may inhibit the growth of specific pathogens in CAC mice by increasing SCFA production, thereby suppressing the occurrence and development of inflammation and tumors.

The synbiotic promotes apoptosis and inhibits proliferation by inhibiting the Wnt/β-catenin signaling pathway

To further explore the potential molecular mechanism of the synbiotic affecting the tumorigenesis and development of CAC, we performed transcriptome sequencing to test colon tissue. Differently expressed genes underwent pathway analysis using KEGG database. The results indicated that the Wnt/β-catenin signaling pathway played a key role in the process that the synbiotic modulated the occurrence and development of CAC (Figure 5A). In addition, the previous results showed that among all the inflammatory factors, IL-23 levels presented the most significant reduction under the synbiotic intervention in the CAC mice. Therefore, we further analyzed the correlation between IL-23 and Wnt/β-catenin signaling pathway based on the value of cor, and cor>0 or cor<0 presented a positive or a negative correlation, respectively. The results demonstrated that IL-23a was positively correlated with 23 genes (including *Dkk2, Notum, Axin2, Nlk, Wif1, Tcf, Ccnd1, Mmp, Wnt 6, Wnt10a, Senp2, Vangl2, Lef 1, Vangl1, Nkd1, Fzd, Wnt16, Wnt3, Bambi, Nfatc3, Wisp1,* and *Gsk3b*), and was negatively correlated with *Sfrp2* gene of Wnt/β-catenin pathway (Table S2).

Furthermore, western blot was performed to verify the results of transcriptome sequencing. We found that the expression of Wnt3a, FZD9 (Frizzled9, a Wnt receptor), and β-catenin in protein level significantly increased in the AOM/DSS group mice, which could be significantly reversed with the synbiotic intervention (Figure 5B). Additionally, the expression of Wnt/β-catenin pathway downstream genes also significantly upregulated in the AOM/DSS group, including transcription factor LEF (lymph enhancement factor) and TCF (T cell factor) (Figure 5B), and target gene c-myc and cyclin D1 (Figure 5C). Moreover, anti-apoptotic protein Bcl-2 (B-cell lymphoma-2) was significantly upregulated and pro-apoptotic protein Bax (BCL2-associated x) was significantly downregulated in the AOM/DSS group (Figure 5C). While the expression of these previously described genes could be reversed under the synbiotic treatment (Figure 5C). Then, we verified the expression of *wnt3a* and *β-catenin* mRNA with qPCR (Figure S8). At the same time, we used IHC staining to detect the expression of the cell proliferation index Ki67, and the positive rate of Ki67 in AOM/DSS group was significantly higher than that in the control group and AOM/DSS_Synbiotic group (Figure 5D).

These above results suggested that in the CAC model mice induced by AOM/DSS, the Wnt/β-catenin signaling pathway is abnormally activated, which promotes the proliferation of cancer cells, inhibits apoptosis, and is accompanied by increased IL-23-mediated inflammation; while the intervention of the synbiotic can suppress the occurrence and development of CAC by inhibiting the activation of this pathway.

DISCUSSION

AOM and DSS are genotoxic and non-genotoxic colonic carcinogens, respectively. Continuous administration of low concentrations of DSS and a certain dose of AOM can produce powerful tumor-promoting activities.[22] To evaluate the effect of the synbiotic in the occurrence of colon cancer, AOM/DSS-induced CAC mouse model was established in this study. The pathological phenotypes, expression levels of tight junction proteins, inflammatory cytokine, and the alterations of intestinal microbes of mice were tested in the present study.

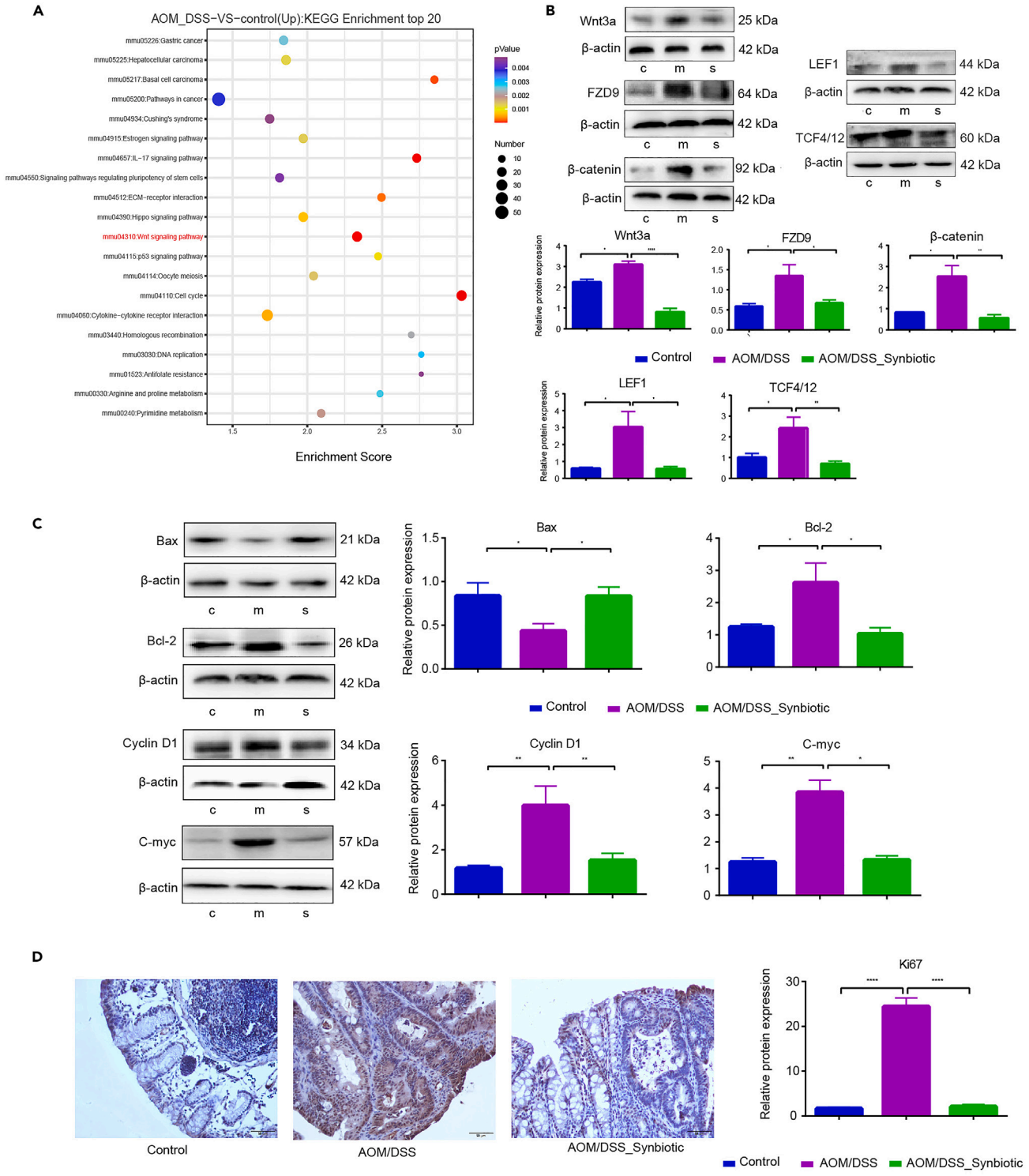

Figure 5. The synbiotic might inhibit the Wnt/β-catenin signaling pathway in mice and inhibit the occurrence and development of tumors

(A) Top-20 bubble chart of mRNA expression in the KEGG enrichment signaling pathway. Transcriptome sequencing of each group of colon tissues, and then based on the KEGG database, the attribution prediction of signal pathways for differentially expressed genes was performed.

(B and C) Western blot was used to verify the expression of key proteins in the Wnt/β-catenin signaling pathway.

(D) IHC analysis of Ki67 expression level (ruler, 50 μm). (The analysis of data is presented as mean ± SEM; *p < 0.05, **p < 0.01, ****p < 0.0001, n = 3–10, Student's *t* test.).

The results showed that compared with control group mice, the AOM/DSS group mice presented lighter weight, shorter colonic length, and colonic tumorigenesis. However, these pathological phenotypes were partly recovered with the synbiotic intervention, which suggested that the synbiotic might inhibit the CAC tumorigenesis. Tight junction protein and inflammatory factors play a crucial role in maintaining cell-to-cell integrity, and increasing intestinal permeability has become an important hallmark of CAC.[23] Intestinal inflammation can obviously affect the function of intestinal epithelial barrier. Intestinal stem cells were exposed to the inflammatory microenvironment that can induce gene mutation, or make stem cells close to the active inflammatory cells that release genotoxic compounds, resulting in the destruction of intestinal barrier,[24] resulting in the increase of molecular infiltration such as lipopolysaccharide (LPS), and then abnormally activate the host immune system, thus aggravating the inflammatory microenvironment.[23] This study found that the expression of ZO-1, occludin, IL-4, and IL-10 was significantly upregulated in AOM/DSS-induced CAC mice and the synbiotic was capable to suppress their expression.

Disturbance of the intestinal microbiota can lead to immune system disorders, thereby promoting the occurrence and development of CAC. The tumor microenvironment formed during the process from intestinal inflammation to CAC will also disrupt the intestinal microecological balance, with an increase in pathogenic bacteria and a decrease in probiotics.[3] Studies have demonstrated that the intestinal microbiota of healthy people was dominated by *Firmicutes*,[25] and *Bacteroides* can damage the barrier function of epithelial cells under certain conditions, which is conducive to the occurrence of chronic inflammation.[26] The ratio of *Bacteroides* to *Firmicutes* (B/F ratio) is an indicator of the health of intestinal microbes.[27,28] In addition, reducing pro-inflammatory cytokines (such as IFN-γ, TNF-α, and IL-1β) and increasing anti-inflammatory cytokines (such as IL-4 and IL-10) can inhibit the occurrence of inflammatory reactions.[29] This study showed that in the gut of CAC mice, the relative abundance of the *phylum Firmicutes* was significantly reduced, the relative abundance of the phylum *Bacteroides* increased, and the (B/F) value significantly raised, indicating that the intestinal microbiota of CAC mice was imbalanced. Further analysis found that some conditional pathogens and pathogenic bacteria such as pathogenic *Escherichia coli*, *Enterotoxigenic Bacteroides fragilis*, and *Shigella* significantly increased in the CAC model group. Correspondingly, the levels of pro-inflammatory cytokines such as TNF-α and IL-1β increased, and the relative abundance of probiotics (such as *Bifidobacterium*, *Lactobacillus*, and *Ruminococcus*) was significantly reduced, which may induce and aggravate the oncogenesis and progress of colorectal cancer. After the synbiotic intervention, the abundance of these probiotics could recover to normal levels, and the expression of anti-inflammatory cytokines IL-4 and IL-10 also increased. The rising of probiotics and anti-inflammatory factors was able to relieve mouse colitis and suppress the tumorigenesis and development of CAC. Therefore, our research also confirmed that the synbiotic can significantly increase the relative abundance of beneficial bacteria and reduce the relative abundance of pathogenic bacteria, thereby alleviating colon inflammation and inhibiting the occurrence of CAC.

Intestinal microorganisms can metabolize host nutrients (such as sugar, fat, and protein) and convert them into a variety of metabolites including SCFAs, amines, secondary bile acids, indole, sulfides, and so on. SCFAs can not only have anti-inflammatory function by regulating the chemotaxis of immune cells, promoting the release of reactive oxygen species and cytokines, but also promote intestinal development by improving intestinal morphology, reducing cell apoptosis, and maintaining the intestinal barrier.[30,31] Additionally, butyric acid can also induce colon cell apoptosis and inhibit colon cancer cell proliferation by blocking histone deacetylase-regulated gene expression.[32] Our results indicated that SCFAs in the colon contents of CAC model mice significantly reduced, which might be related to the decrease of SCFA-producing bacteria. After the synbiotic intervention, butyric acid-producing bacteria and SCFAs significantly increased in AOM/DSS mice, thereby inhibiting the occurrence of inflammatory reactions, preventing the destruction of the intestinal barrier and inhibiting the occurrence of CAC. Tryptophan can be converted into indole-containing molecules with biological activity by bacteria, which activate aryl hydrocarbon receptors and downregulate the production of inflammatory cytokines, improve intestinal barrier function, and suppress colon inflammation.[33–35] The intestinal symbiosis *Peptostreptococcus* can produce special indole derivative indole propionic acid, induce mucin gene expression, and activate the NRF2 pathway to inhibit intestinal inflammation.[33] *Bacteroides* can metabolize tryptophan into the precursor of serotonin that can function multiple effects by binding to different 5-hydroxytryptamine (5-HT) receptors and regulate intestinal inflammation.[36] The present study showed that compared with the normal group mice, tryptophan and 5-HT significantly accumulated, and tryptophan metabolites IAA, IPA, and IA levels significantly dropped in the colon contents of CAC model mice. However, this study showed that the

imbalanced microbial tryptophan metabolism was significantly restored under the synbiotic intervention, which may be attributed to the intervention of intestinal microbes in tryptophan metabolism. Previous studies revealed that tryptophan metabolism was able to improve the intestinal barrier function and activate the immune system.[37] Primary bile acids are produced by the host and are modified by bacteria such as *Lactobacillus* and *Bifidobacterium* to form secondary bile acids with anti-inflammatory activity.[38] High concentration of primary bile acid (deoxycholic acid) can inhibit the growth of *Lactobacillus* and *Bifidobacterium*, and promote the occurrence of intestinal tumors.[39] This study demonstrated that compared with the normal control group, the primary bile acid in the colon content of the CAC mouse model group significantly enriched, and the secondary bile acid level significantly reduced. While under the treatment of the synbiotic, the levels of intestinal metabolites could gradually return to normal levels, which might be related to the increasing relative abundance of *lactobacilli* and *bifidobacteria*.

Abnormal activation of Wnt/β-catenin signaling pathway is considered to be the main factor leading to the oncogenesis of CRC.[40] This study found that the expression of Wnt3a was significantly increased in the CAC model group mice. The expression of the transmembrane frizzled receptor (FZD9) was significantly upregulated, and β-catenin was significantly accumulated in the nucleus. The expression of TCF/LEF transcription factors in the nucleus was also significantly increased, which started and enhanced the expression of downstream target genes cyclin D1, c-Myc. However, the synbiotic intervention could significantly promote the expression of intestinal mucosa-related proteins and inhibit the activation of Wnt/β-catenin signaling pathway. Previously, Neurath et al. suggested that colon cancer growth could be regulated by affecting the expression of IL-23R. Our results also showed that upregulation of IL-23 was significantly associated with activation of the Wnt/β-catenin signaling pathway.[41] It has also been shown that the use of probiotic *L. rhamnosus GG* reduces the expression of NF-κB, β-catenin, and COX-2 in colon cancer tissues.[42] Moreover, activation of the Wnt signaling pathway is associated with the expression of cytokines, leading to the upregulation of the pro-inflammatory cytokine TNF-α,[43] and the upregulated TNF-α in turn can induce the expression of β-catenin.[44] Our results also showed that the expression of TNF-α was upregulated and Wnt signaling pathway was activated in the intestine of CAC mice, which could be reversed after supplementing the synbiotic. Thus, we speculated that the probiotics might regulated TNF-α expression via Wnt signaling pathway in this study, which need further be verified. In summary, these above results suggested that the probiotics may exert antitumor effects by inhibiting the activation of Wnt/β-catenin signaling pathway by regulating the inflammatory response.

This study confirmed that the synbiotic supplementation could inhibit the intestinal barrier damage and the occurrence of intestinal cancer in CAC mice. The synbiotic supplementation significantly upregulated the expression of tight junction proteins including ZO-1, occludin, and anti-inflammatory cytokines, and downregulated the expression of pro-inflammatory cytokines. Moreover, the synbiotic significantly improved colonic microbiota disorder of CAC mice, and promoted the production of SCFAs and secondary bile acids, and alleviated the accumulation of primary bile acids in the intestinal contents of AOM/DSS mice. Finally, the synbiotic could significantly inhibit the abnormal activation of intestinal Wnt/β-catenin signaling pathway. This study suggested that the synbiotic may be a functional food to prevent inflammation-related colon tumors, and also provided a theoretical basis for improving the intestinal microecological environment through diet therapy.

Limitations of the study

In this study, there exist some limitations. Firstly, the effect of inflammatory factors (such as TNF-α and IL-23) on the activation of Wnt/β-catenin signaling pathway should be further investigated. Secondly, the experiment was only performed on mice and without cells data, which are more meaningful for the application of the synbiotic. Thirdly, this did not further reveal the effect and mechanism of the differential metabolites caused by key differential bacteria to immune system or Wnt/β-catenin signaling pathway.

STAR★METHODS

Detailed methods are provided in the online version of this paper and include the following:

- KEY RESOURCES TABLE
- RESOURCE AVAILABILITY
  - Lead contact
  - Materials availability

SUPPLEMENTAL INFORMATION

Supplemental information can be found online at https://doi.org/10.1016/j.isci.2023.106979.

ACKNOWLEDGMENTS

This work was supported by the National Natural Science Foundation of China (No. 31072141), the Scientific Research Fund of Hunan Provincial Education Department (No. 2019A293), and Hunan Provincial Key Research and Development Program (No. 2019SK2042).

AUTHOR CONTRIBUTIONS

H.W., Z.W., and Y.Q. contributed to animal feeding, material preparation, experiments performing, and the sequencing data analysis; Z.Z., Y.Z., M.L., F.Z., and J.C. contributed to some experiments, statistical analysis of data, and supervised the project.; R.L. conceived and designed the experiments, funding acquisition, and wrote the paper. All authors read and approved the final manuscript.

DECLARATION OF INTERESTS

The authors declare no competing interests.

INCLUSION AND DIVERSITY

We support inclusive, diverse, and equitable conduct of research.

Received: July 9, 2022
Revised: April 11, 2023
Accepted: May 24, 2023
Published: May 28, 2023

REFERENCES

1. Keum, N., and Giovannucci, E. (2019). Global burden of colorectal cancer: emerging trends, risk factors and prevention strategies. Nat. Rev. Gastroenterol. Hepatol. *16*, 713–732. https://doi.org/10.1038/s41575-019-0189-8.

2. GBD 2017 Colorectal Cancer Collaborators (2019). The global, regional, and national burden of colorectal cancer and its attributable risk factors in 195 countries and territories, 1990-2017: a systematic analysis for the Global Burden of Disease Study 2017. Lancet. Gastroenterol. Hepatol. *4*, 913–933. https://doi.org/10.1016/S2468-1253(19)30345-0.

3. Janney, A., Powrie, F., and Mann, E.H. (2020). Host-microbiota maladaptation in colorectal cancer. Nature *585*, 509–517. https://doi.org/10.1038/s41586-020-2729-3.

4. Jess, T., Rungoe, C., and Peyrin-Biroulet, L. (2012). Risk of colorectal cancer in patients with ulcerative colitis: a meta-analysis of population-based cohort studies. Clin. Gastroenterol. Hepatol. *10*, 639–645. https://doi.org/10.1016/j.cgh.2012.01.010.

5. Vendramini-Costa, D.B., and Carvalho, J.E. (2012). Molecular link mechanisms between inflammation and cancer. Curr. Pharm. Des. *18*, 3831–3852. https://doi.org/10.2174/138161212802083707.

6. van Staa, T.P., Card, T., Logan, R.F., and Leufkens, H.G.M. (2005). 5-Aminosalicylate use and colorectal cancer risk in inflammatory bowel disease: a large epidemiological study. Gut *54*, 1573–1578. https://doi.org/10.1136/gut.2005.070896.

7. Sada, O., Ahmed, K., Jeldo, A., and Shafi, M. (2020). Role of anti-inflammatory drugs in the colorectal cancer. Hosp. Pharm. *55*, 168–180. https://doi.org/10.1177/0018578718823736.

8. Gibson, G.R., and Roberfroid, M.B. (1995). Dietary modulation of the human colonic microbiota: introducing the concept of prebiotics. J. Nutr. *125*, 1401–1412. https://doi.org/10.1093/jn/125.6.1401.

9. Gibson, G.R., Hutkins, R., Sanders, M.E., Prescott, S.L., Reimer, R.A., Salminen, S.J., Scott, K., Stanton, C., Swanson, K.S., Cani, P.D., et al. (2017). Expert consensus

document: the International Scientific Association for Probiotics and Prebiotics (ISAPP) consensus statement on the definition and scope of prebiotics. Nat. Rev. Gastroenterol. Hepatol. *14*, 491–502. https://doi.org/10.1038/nrgastro.2017.75.

10. Shi, Y., Zhai, Q., Li, D., Mao, B., Liu, X., Zhao, J., Zhang, H., and Chen, W. (2017). Restoration of cefixime-induced gut microbiota changes by Lactobacillus cocktails and fructooligosaccharides in a mouse model. Microbiol. Res. *200*, 14–24. https://doi.org/10.1016/j.micres.2017.04.001.

11. Lloyd-Price, J., Abu-Ali, G., and Huttenhower, C. (2016). The healthy human microbiome. Genome Med. *8*, 51. https://doi.org/10.1186/s13073-016-0307-y.

12. Pan, T., Guo, H.Y., Zhang, H., Liu, A.P., Wang, X.X., and Ren, F.Z. (2014). Oral administration of Lactobacillus paracasei alleviates clinical symptoms of colitis induced by dextran sulphate sodium salt in BALB/c mice. Benef. Microbes *5*, 315–322. https://doi.org/10.3920/BM2013.0041.

13. Li, Q., Hu, W., Liu, W.X., Zhao, L.Y., Huang, D., Liu, X.D., Chan, H., Zhang, Y., Zeng, J.D., Coker, O.O., et al. (2021). Streptococcus thermophilus inhibits colorectal tumorigenesis through secreting beta-galactosidase. Gastroenterology *160*, 1179–1193.e14. https://doi.org/10.1053/j.gastro.2020.09.003.

14. Shimizu, K., Yamada, T., Ogura, H., Mohri, T., Kiguchi, T., Fujimi, S., Asahara, T., Yamada, T., Ojima, M., Ikeda, M., and Shimazu, T. (2018). Synbiotics modulate gut microbiota and reduce enteritis and ventilator-associated pneumonia in patients with sepsis: a randomized controlled trial. Crit. Care *22*, 239. https://doi.org/10.1186/s13054-018-2167-x.

15. Greenhalgh, K., Ramiro-Garcia, J., Heinken, A., Ullmann, P., Bintener, T., Pacheco, M.P., Baginska, J., Shah, P., Frachet, A., Halder, R., et al. (2019). Integrated in vitro and in silico modeling delineates the molecular effects of a synbiotic regimen on colorectal-cancer-derived cells. Cell Rep. *27*, 1621–1632.e9. https://doi.org/10.1016/j.celrep.2019.04.001.

16. Liao, M., Zhang, Y., Qiu, Y., Wu, Z., Zhong, Z., Zeng, X., Zeng, Y., Xiong, L., Wen, Y., and Liu, R. (2021). Fructooligosaccharide supplementation alleviated the pathological immune response and prevented the impairment of intestinal barrier in DSS-induced acute colitis mice. Food Funct. *12*, 9844–9854. https://doi.org/10.1039/d1fo01147b.

17. Ford, A.C., Sperber, A.D., Corsetti, M., and Camilleri, M. (2020). Irritable bowel syndrome. Lancet *396*, 1675–1688. https://doi.org/10.1016/S0140-6736(20)31548-8.

18. Chen, F., Dai, X., Zhou, C.C., Li, K.X., Zhang, Y.J., Lou, X.Y., Zhu, Y.M., Sun, Y.L., Peng, B.X., and Cui, W. (2022). Integrated analysis of the faecal metagenome and serum metabolome reveals the role of gut microbiome-associated metabolites in the detection of colorectal cancer and adenoma. Gut *71*, 1315–1325. https://doi.org/10.1136/gutjnl-2020-323476.

19. Yang, J., Wei, H., Zhou, Y., Szeto, C.H., Li, C., Lin, Y., Coker, O.O., Lau, H.C.H., Chan, A.W.H., Sung, J.J.Y., and Yu, J. (2022). High-fat diet promotes colorectal tumorigenesis through modulating gut microbiota and metabolites. Gastroenterology *162*, 135–149.e2. https://doi.org/10.1053/j.gastro.2021.08.041.

20. LeBlanc, J.G., Chain, F., Martín, R., Bermúdez-Humarán, L.G., Courau, S., and Langella, P. (2017). Beneficial effects on host energy metabolism of short-chain fatty acids and vitamins produced by commensal and probiotic bacteria. Microb. Cell Fact. *16*, 79. https://doi.org/10.1186/s12934-017-0691-z.

21. Sun, Y., and O'Riordan, M.X.D. (2013). Regulation of bacterial pathogenesis by intestinal short-chain fatty acids. Adv. Appl. Microbiol. *85*, 93–118. https://doi.org/10.1016/B978-0-12-407672-3.00003-4.

22. De Robertis, M., Massi, E., Poeta, M.L., Carotti, S., Morini, S., Cecchetelli, L., Signori, E., and Fazio, V.M. (2011). The AOM/DSS murine model for the study of colon carcinogenesis: from pathways to diagnosis and therapy studies. J. Carcinog. *10*, 9. https://doi.org/10.4103/1477-3163.78279.

23. Lasry, A., Zinger, A., and Ben-Neriah, Y. (2016). Inflammatory networks underlying colorectal cancer. Nat. Immunol. *17*, 230–240. https://doi.org/10.1038/ni.3384.

24. Xavier, R.J., and Podolsky, D.K. (2007). Unravelling the pathogenesis of inflammatory bowel disease. Nature *448*, 427–434. https://doi.org/10.1038/nature06005.

25. Murri, M., Leiva, I., Gomez-Zumaquero, J.M., Tinahones, F.J., Cardona, F., Soriguer, F., and Queipo-Ortuño, M.I. (2013). Gut microbiota in children with type 1 diabetes differs from that in healthy children: a case-control study. BMC Med. *11*, 46. https://doi.org/10.1186/1741-7015-11-46.

26. Tlaskalová-Hogenová, H., Stěpánková, R., Kozáková, H., Hudcovic, T., Vannucci, L., Tučková, L., Rossmann, P., Hrnčíř, T., Kverka, M., Zákostelská, Z., et al. (2011). The role of gut microbiota (commensal bacteria) and the mucosal barrier in the pathogenesis of inflammatory and autoimmune diseases and cancer: contribution of germ-free and gnotobiotic animal models of human diseases. Cell. Mol. Immunol. *8*, 110–120. https://doi.org/10.1038/cmi.2010.67.

27. Li, W., and Ma, Z.S. (2020). FBA ecological guild: trio of firmicutes-bacteroidetes alliance against actinobacteria in human oral microbiome. Sci. Rep. *10*, 287. https://doi.org/10.1038/s41598-019-56561-1.

28. Tseng, C.H., and Wu, C.Y. (2019). The gut microbiome in obesity. J. Formos. Med. Assoc. *118*, S3–S9. https://doi.org/10.1016/j.jfma.2018.07.009.

29. Xu, L., Guo, Y., Zhao, Y., Xu, Y., Peng, X., Yang, Z., Tao, R., Huang, Y., Xu, Y., Chen, Y., and Zhu, B. (2019). Chemokine and cytokine cascade caused by skewing of the Th1-Th2 balance is associated with high intracranial pressure in HIV-associated cryptococcal meningitis. Mediat. Inflamm. *2019*, 2053958. https://doi.org/10.1155/2019/2053958.

30. Śliżewska, K., Markowiak-Kopeć, P., and Śliżewska, W. (2020). The role of probiotics in cancer prevention. Cancers *13*, 20. https://doi.org/10.3390/cancers13010020.

31. Sun, M., Wu, W., Liu, Z., and Cong, Y. (2017). Microbiota metabolite short chain fatty acids, GPCR, and inflammatory bowel diseases. J. Gastroenterol. *52*, 1–8. https://doi.org/10.1007/s00535-016-1242-9.

32. Steliou, K., Boosalis, M.S., Perrine, S.P., Sangerman, J., and Faller, D.V. (2012). Butyrate histone deacetylase inhibitors. Biores. Open Access *1*, 192–198. https://doi.org/10.1089/biores.2012.0223.

33. Venkatesh, M., Mukherjee, S., Wang, H., Li, H., Sun, K., Benechet, A.P., Qiu, Z., Maher, L., Redinbo, M.R., Phillips, R.S., et al. (2014). Symbiotic bacterial metabolites regulate gastrointestinal barrier function via the xenobiotic sensor PXR and Toll-like receptor 4. Immunity *41*, 296–310. https://doi.org/10.1016/j.immuni.2014.06.014.

34. Zelante, T., Iannitti, R.G., Cunha, C., De Luca, A., Giovannini, G., Pieraccini, G., Zecchi, R., D'Angelo, C., Massi-Benedetti, C., Fallarino, F., et al. (2013). Tryptophan catabolites from microbiota engage aryl hydrocarbon receptor and balance mucosal reactivity via interleukin-22. Immunity *39*, 372–385. https://doi.org/10.1016/j.immuni.2013.08.003.

35. Wlodarska, M., Luo, C., Kolde, R., d'Hennezel, E., Annand, J.W., Heim, C.E., Krastel, P., Schmitt, E.K., Omar, A.S., Creasey, E.A., et al. (2017). Indoleacrylic acid produced by commensal peptostreptococcus species suppresses inflammation. Cell Host Microbe *22*, 25–37.e6. https://doi.org/10.1016/j.chom.2017.06.007.

36. Kannen, V., Bader, M., Sakita, J.Y., Uyemura, S.A., and Squire, J.A. (2020). The dual role of serotonin in colorectal cancer. Trends Endocrin Met *31*, 611–625. https://doi.org/10.1016/j.tem.2020.04.008.

37. Roager, H.M., and Licht, T.R. (2018). Microbial tryptophan catabolites in health and disease. Nat. Commun. *9*, 3294. https://doi.org/10.1038/s41467-018-05470-4.

38. Jia, W., Xie, G., and Jia, W. (2018). Bile acid-microbiota crosstalk in gastrointestinal inflammation and carcinogenesis. Nat. Rev. Gastroenterol. Hepatol. *15*, 111–128. https://doi.org/10.1038/nrgastro.2017.119.

39. Janssen, A.W.F., Houben, T., Katiraei, S., Dijk, W., Boutens, L., van der Bolt, N., Wang, Z., Brown, J.M., Hazen, S.L., Mandard, S., et al. (2017). Modulation of the gut microbiota impacts nonalcoholic fatty liver disease: a potential role for bile acids. J. Lipid Res. *58*, 1399–1416. https://doi.org/10.1194/jlr.M075713.

40. Sebio, A., Kahn, M., and Lenz, H.J. (2014). The potential of targeting Wnt/beta-catenin in colon cancer. Expert Opin. Ther. Targets *18*, 611–615. https://doi.org/10.1517/14728222.2014.906580.

41. Neurath, M.F. (2019). IL-23 in inflammatory bowel diseases and colon cancer. Cytokine Growth Factor Rev. *45*, 1–8. https://doi.org/10.1016/j.cytogfr.2018.12.002.

42. Kaeid Sharaf, L., and Shukla, G. (2018). Probiotics (Lactobacillus acidophilus and Lactobacillus rhamnosus GG) in conjunction with celecoxib (selective COX-2 inhibitor) modulated DMH-induced early experimental colon carcinogenesis. Nutr. Cancer *70*, 946–955. https://doi.org/10.1080/01635581.2018.1490783.

43. Zhou, Y.Q., Tian, X.B., Tian, Y.K., Mei, W., Liu, D.Q., and Ye, D.W. (2022). Wnt signaling: a prospective therapeutic target for chronic pain. Pharmacol. Ther. *231*, 107984. https://doi.org/10.1016/j.pharmthera.2021.107984.

44. Zhao, Y., Wang, C., Hong, X., Miao, J., Liao, Y., Hou, F.F., Zhou, L., and Liu, Y. (2019). Wnt/beta-catenin signaling mediates both heart and kidney injury in type 2 cardiorenal syndrome. Kidney Int. *95*, 815–829. https://doi.org/10.1016/j.kint.2018.11.021.

45. Zheng, J., Wittouck, S., Salvetti, E., Franz, C.M.A.P., Harris, H.M.B., Mattarelli, P., O'Toole, P.W., Pot, B., Vandamme, P., Walter, J., et al. (2020). A taxonomic note on the genus Lactobacillus: description of 23 novel genera, emended description of the genus Lactobacillus Beijerinck 1901, and union of Lactobacillaceae and Leuconostocaceae. Int. J. Syst. Evol. Microbiol. *70*, 2782–2858. https://doi.org/10.1099/ijsem.0.004107.

STAR★METHODS

KEY RESOURCES TABLE

REAGENT or RESOURCE	SOURCE	IDENTIFIER
Antibodies		
Beta Actin Polyclonal antibody	Proteintech	Cat# 20536-1-AP; RRID: AB_1-700003
TNF Alpha Monoclonal antibody	Proteintech	Cat# 60291-1-Ig; RRID:AB_2833255
Occludin Polyclonal antibody	Proteintech	Cat# 27260-1-AP; RRID:AB_2880820
ZO-1 Polyclonal antibody	Proteintech	Cat# 21773-1-AP; RRID:AB_10733242
IL23 Monoclonal antibody	Abmart	Cat# T58544 RRID:AB_2935661
Wnt3 Monoclonal antibody	Abmart	Cat# TD13430 RRID:AB_2935662
FZD9 Monoclonal antibody	Abmart	Cat# TP72258S RRID:AB_2935663
β-catenin Monoclonal antibody	Abmart	Cat# T53523S RRID:AB_2935664
LEF1 Monoclonal antibody	Abmart	Cat# T55350 RRID:AB_2935665
TCF4/12 Monoclonal antibody	Abmart	Cat# TP74355 RRID:AB_2935666
Bax Monoclonal antibody	Abmart	Cat# T40051 RRID:AB_2910262
Bcl-2 Monoclonal antibody	Abmart	Cat# T40056 RRID:AB_2929011
C-myc Monoclonal antibody	Abmart	Cat# T55150 RRID:AB_2934184
Ki67 Monoclonal antibody	Signalway Antibody (SAB)	Cat# 38019 RRID:AB_2935682
Bacterial and virus strains		
Lactobacillus acidophilus TYCA06	Hunan Tian'an Biotechnology Co., LTD	NA
Lacticaseibacillus rhamnosus F-1	Hunan Tian'an Biotechnology Co., LTD	NA
Bifidobacterium adolescentis BH-20	Hunan Tian'an Biotechnology Co., LTD	NA
Bifidobacterium longum BB536	Hunan Tian'an Biotechnology Co., LTD	NA
Bifidobacterium animalis bb12	Hunan Tian'an Biotechnology Co., LTD	NA
Limosilactobacillus reuteri GL-104	Hunan Tian'an Biotechnology Co., LTD	NA
Lactobacillus bulgaricus 11842	Hunan Tian'an Biotechnology Co., LTD	NA
Streptococcus thermophilus	Hunan Tian'an Biotechnology Co., LTD	NA
Chemicals, peptides, and recombinant proteins		
AOM	Sigma-Aldrich	A5486
DSS	MP Biomedicals	160110
Critical commercial assays		
FOS	Shaoshan Changbaitong Biotechnology Co., LTD	P95S
HE dye solution set	Servicebio	G1003
DAB	Servicebio	ZLI-9017
BCA kit	CWBIO Co. Ltd	CW0014S
ECL chemiluminescence solution	Monad Biotech. Co. Ltd.	130231
TRIzol reagen	BeijingDing-guo-chang-sheng Biological	NEP019
*Evo M-MLV*RT Kit with gDNA Clean for qPCR	Accurate Biology	AG11705
SYBR® Green Premix *Pro Taq* HS qPCR Kit	Accurate Biology	AG11701
DNeasy PowerSoil Kit	QIAGEN	12888
QIAamp 96 PowerFecal QIAcube HT kit	QIAGEN	51531
Qubit dsDNA Assay Kit	Life Technologies	Q32854
Tks Gflex DNA Polymerase	Takara	R060B

(*Continued on next page*)

Continued

REAGENT or RESOURCE	SOURCE	IDENTIFIER
mirVana™ miRNA ISOlation Kit	Ambion	1561
Trustee Stranded mRNA LTSample Prep Kit	Illumina	RS-122-2101
Deposited data		
16S rRNA gene sequencing data	This paper	NCBI: SAMN23929712
Experimental models: Organisms/strains		
Balb/cSlac,mus musculus	SLAC LABORATORY ANIMAL	NA
Oligonucleotides		
Primers for *gapdh*, *occludin*, *ZO-1*, *COX-2*, *Tnf-α*, *Il17A*, *Il23*, *Il12b*, *Il1β*, *Il4*, *Il10*, *wnt3a*, *β-catenin*, see Table S1	This paper	N/A
Software and algorithms		
Image J	https://imagej.nih.gov/ij/	NA
Trimmomatic	http://www.usadellab.org/cms/?page=trimmomatic	version 0.35
FLASH	http://www.flash.cn	version 1.2.11
QIIME split_libraries	http://qiime.org/scripts/split_libraries.html	version 1.8.0
UCHIME	http://drive5.com/uchime/uchime_download.html	version 2.4.2
Vsearch	https://github.com/torognes/vsearch/releases	version 2.4.2
Trimmomatic	http://www.usadellab.org/cms/?page=trimmomatic	Version 0.36
Hisat 2	http://daehwankimlab.github.io/hisat2/download/	Version 2.2.1.0
DESeq	https://www.bioconductor.org/packages//2.10/bioc/html/DESeq.html	Version 1.18.0
Progenesis QI	https://www.nonlinear.com/progenesis/qi/download/	Version 2.3
GraphPad Prism	https://www.graphpad.com/	Version 6.01
Other		
KEGG Database	https://www.kegg.jp/	NA

RESOURCE AVAILABILITY

Lead contact

Further information and requests for resources and reagents should be directed to and will be fulfilled by the lead contact, Rushi Liu (liurushi@hunnu.edu.cn).

Materials availability

This study did not generate new unique reagents.

Data and code availability

- 16S rDNA gene sequencing data have been deposited at NCBI and are publicly available as of the date of publication. The accession number is SAMN23929712.
- The original codes are deposited in NCBI with this link: NCBI: https://submit.ncbi.nlm.nih.gov/subs/sra/SUB10792714/overvie, Sequence Read Archive (SRA) submission: SUB10792714.

- Any additional information required to reanalyze the data reported in this paper is available from the lead contact upon request.

EXPERIMENTAL MODEL AND SUBJECT DETAILS

Mice

Healthy male Balb/c mice (6-week-old) were obtained from SLAC LABORATORY ANIMAL. Animal study protocols were approved by the ethics committee Board of Hunan Normal University. All animals were housed under specific pathogen-free (SPF) conditions according to the National Institutes of Health's Guide for the Care and Use of Laboratory Animals (NIH Publications no. 8023, revised 1978).

METHOD DETAILS

Synbiotic

The synbiotic applied in this study was constituted of FOS (P95S) By Changsha Tian'an Biotechnology Co., LTD and 8 probiotic strains, including *Lactobacillus acidophilus* TYCA06, *Lacticaseibacillus rhamnosus* F-1, *Limosilactobacillus reuteri* GL-104, *Lactobacillus bulgaricus* 11842,[45] *Bifidobacterium adolescentis* BH-20, *Bifidobacterium longum* BB536, *Bifidobacterium animalis* bb12, and *Streptococcus thermophilus By Shaoshan Changbaitong Biotechnology Co., LTD*. Finally, the FOS and the probiotics were evenly mixed under aseptic conditions to obtain the specific synbiotic used in this study.[16]

Mouse models

After a week of adaptation to the laboratory conditions, the mice were assigned to three groups, as Control group, AOM/DSS-induced CAC group (AOM/DSS), and synbiotic-treated CAC group (AOM/DSS_Synbiotic) (n=10). The AOM/DSS group and AOM/DSS_Synbiotic group were given a single intraperitoneal injection of 10 mg/kg AOM (Sigma-Aldrich, A5486), then administered 2.5% DSS drinking water on the 2nd, 5th and 8th week of the experiment, and given routine aqueous solution provided at other time.[22] Based on our experience in previous studies,[16] the mice in AOM/DSS_Synbiotic group were daily administered with the synbiotic (FOS 2 g/kg b.w. + probiotics 10^9 CFU/kg b.w.) by gavage every day (this dose was well-tolerated for weeks of administration in adult inbred mice and had no significant effect on health status.), and mice of the other two groups were gavaged with sterilized water. During this period, all the mice were fed with ordinary rodent fodder. Body weight was weighed once a day. At the 10th week, the mice were euthanized, and the colon was collected and measured, and then the colon was cut longitudinally and the intestinal contents were collected for metabolism analysis. Finally, washed the colon with PBS, counted the number of tumors and measured the diameter. The 2 cm colon under the caecum was cut out as specimens for microbiota detection and transcriptome sequencing, and the distal 1 cm colon was cut and fixed with 10% formalin. Protein or RNA were extracted from the rest of the intestine, and performed Western blot or quantitative PCR analysis.

Histopathological analysis

The colon tissues were embedded in paraffin. 3 μm-thick sections were sliced from routinely with a semi-automatic paraffin microtome for hematoxylin-eosin staining (HE staining) and immunohistochemistry. HE staining were performed as previously described.[16] Briefly, 3 μm-thick sections were de-paraffinized with xylene solutions I and II (each for 10 min), rehydrated through anhydrous ethanol I and II, 95% alcohol, and 85% alcohol (each for 5 min) in sequence, rinsed with tap water for 5 min; and then counterstained with hematoxylin for 5 min, dehydrated with 85% alcohol for 1 min and counterstained with eosin for 3 min. Following, the sections were placed in 80% alcohol, 90% alcohol, and absolute ethanol I and II (each for 1 min) for dehydration. After the slices were air-dried, make it transparent with xylene for 5 min and seal with neutral gum. The number of mice samples in each group is not less than 5, and each mouse randomly selected more than 5 fields of view under a 20-fold objective lens for analysis. The images were captured by an optical microscope and evaluated by two independent researchers.

Immunohistochemistry (IHC) analysis

Ki67 expression was determined by immunohistochemistry. 3 μm-thick sections were removed with xylene, rehydrated with graded alcohols, and then treated with 0.01M sodium citrate for antigen retrieval. Sections were incubated with 3% hydrogen peroxide for 15 min in the dark to quench endogenous peroxidase activity, and then incubated with goat serum for 30 min at room temperature for blocking. Sections were

incubated with primary antibody (diluted 1:300) at 4°C, and then rinsed four times with PBST. Then, these sections were incubated with HRP-conjugated secondary antibodies (diluted 1:1000) for 45 min at 37°C, rinsed four times with PBST again. DAB (ZLI-9017, ZSGB BiioCo.Ltd., Beijing, China) was added for 1 min and immediately were terminated with tap water after color development. The slides were washed four times with PBST and counter stained with hematoxylin for 90s. The sections were finally dehydrated in graded alcohols, soaked in xylene, and fixed in neutral balsam. The pictures were taken by a light microscope (Olympus CX41) and the optical density was analyzed by using the Image J software (https://imagej.nih.gov/ij/).

Western blot analysis

The tissue lysate was added to the mouse colon according to 200 μL/10 mg tissue standard. The tissue lysate was fully ground on ice with a tissue homogenizer, and then stood for 30 min to fully lyse the tissue. Then the supernatant was centrifuged at 12000 g at 4°C for 15 min, and the supernatant was collected. The BCA kit (CW0014S, CWBIO Co. Ltd) was applied to determine the concentration of the protein sample, SDS-PAGE electrophoresis was performed, and then the proteins on the gel was transferred to the PVDF membrane. Then the PVDF membrane was put into a heat-sealable plastic bag with 5 mL of 5% skimmed milk, for 1.5 h at room temperature. After blocking, the membranes were incubated with primary antibody (diluted as 1:1000) against at 4°C overnight, and was washed in TBST (100 mmol/L Tris·HCl, 0.9% (m/V) NaCl, 0.2% Tween 20, pH 7.5) 3 times for 5 min each. Following, PVDF membrane was incubated in the enzyme-conjugated secondary antibody (at a dilution of 1:5000 (goat anti-rabbit IgG, AP132P, Millipore Co. Ltd.; goat anti-mouse IgG, abs20001, Absin Bioscience Co. Ltd., China) at room temperature for 40 min, and was washed in TBST buffer 3 times for 5 min each. The PVDF membrane was dropped with ECL chemiluminescence solution (130231, Monad Biotech. Co. Ltd., China), and scanned with Tanon 5500 system (Tanon Co. Ltd., Shanghai, China) to develop specific protein band. Finally, the quantitation analysis was performed using ImageJ software and normalized to β-actin band intensity on the same membrane. The primary antibody against β-actin, Occludin, ZO-1 and TNF-α were purchased from Proteintech Inc., China, and the other primary antibodies were purchased from Abmart medical technology (Shanghai) Co., Ltd, China.

Real-time fluorescence quantitative PCR analysis

TRIzol reagent was used (Beijing Ding-guo-chang-sheng Biological, China) to extract total RNA according to the kit instructions. Then the RNA was quantified using SynergyHTX microplate reader (Borton, USA), and then cDNA synthesis was performed using *Evo M-MLV* RT Kit with gDNA Clean for qPCR (Accurate Biology, China). Real-time fluorescent quantitative PCR was performed with SYBR Green Premix *Pro Taq* HS qPCR Kit (Accurate Biology, China) on CFX96™ quantitative PCR instrument (Bio-Rad). The primer sequence was shown in Table S1. The data of the real-time fluorescence quantitative PCR was analyzed by the $2^{-\Delta\Delta Ct}$ method, and the data was normalized by the results of *GAPDH* gene amplification.

Microbial community analysis

The mouse colon mucosal tissue microbes were isolated and the total genomic DNA was extracted with QIAGEN DNA Extraction kit following the instructions. Extracted DNA was diluted to a concentration of 1 ng/μL, and Extracted DNA was diluted to a concentration of 1 ng/ul and used as template for PCR amplification of bacterial 16s rDNA with barcoded primers and Takara Ex Taq (Takara) for amplicon sequencing. The 16s rDNA V3-V4 variable region was amplified using universal primers 343F and 798R. After 2 rounds of PCR, the final amplicons were purified with AMPure XP beads (Agcourt), and Quantification was performed using the Qubit dsDNA kit. Equal amounts of purified amplicon were pooled for subsequent sequencing on Illumina MiSeq, conducted by OE Biotech Company (Shanghai, China). The Trimmomatic software (version 0.35) was used to remove the original double-end sequence, and the FLASH (version 1.2.11) software was used to splice the double-ended sequence after the removal. The maximum overlap during sequence splicing was 200 bp, and the complete paired end sequence was obtained. Then the split_libraries (version 1.8.0) software in QIIME was used to remove the sequence containing N bases in the paired end sequence, the sequence with single base repeat greater than 8 was removed, the sequence with length less than 200bp was removed, and the clean tags sequence was obtained. Then UCHIME (version 2.4.2) software was applied to remove the chimera in clean tags, and finally valid tags were obtained for OTU division later. After the sequencing data was preprocessed to generate high-quality sequences, Vsearch software (version 2.4.2) was used to classify the sequences into multiple OTUs based on the 97% similarity of the sequences. QIIME software was used to select the representative sequences of each OTU, and all

representative sequences were compared with the database Greengenes. RDP classifier software was used to annotate and compare (0.7 confidence values as cutoff). The samples were analyzed for Alpha diversity and Beta diversity.

Transcriptome analysis of intestinal mucosa

The total RNA of the samples was extracted using mirVana™ miRNA ISOlation Kit (Ambion-1561), and the DNA in the sample was digested with DNase, and then Oligo (dT) magnetic beads were used to enrich the mRNA. The Trustee Stranded mRNA LTSample Prep Kit (Illumina, RS-122-2101) was used to purify the mRNA, then the mRNA was split into fragments. The first strand cDNA with six base random primers was synthesized, and then the second strand cDNA was synthesized and purified. The purified double-stranded cDNA was then repaired, and added with A tail, and then connected to the sequencing adapter. Then, the appropriate fragment size was selected. Finally, PCR amplification was performed. After the constructed library was qualified by the Agilent 2100 Bioanalyzer, it was sequenced using the Illumina HiSeqTM 2500 sequencer to generate 125 bp or 150 bp paired-end data. The sequencing and transcriptome analysis were conducted by OE Biotech Company (Shanghai, China). In order to obtain high-quality reads that could be used for subsequent analysis, further quality filtering was performed on raw reads. Firstly, Trimmomatic software (Version 0.36) was used for quality control and the adapters were removed, then low-quality bases and N-bases were filtered out, and finally high-quality clean reads were obtained. Hisat 2(Version 2.2.1.0) software were applied to compare clean reads to the reference genome of the species, and evaluate the sample based on the genome comparison rate. The result of comparing clean reads with the reference genome was stored in a binary file. The gene FPKM expression value was quantified using cufflinks software. When calculating the difference in gene expression, the number of reads that fall into each sample was obtained through the htseqcount software, and the estimated Size Factors function of the DESeq (Version 1.18.0) R package is used to normalize the data, and the nbinom.test function was used to calculate the p value and foldchange value of the difference comparison. The differential genes with a p value of less than 0.05 and a multiple of difference greater than 2 was selected, and the KEGG (http://www.genome.jp/kegg/) enrichment analysis of the differential genes was performed to determine the biological functions or pathways that the differential genes mainly affect. At the same time, unsupervised hierarchical clustering of differential genes was performed, and the expression patterns of differential genes among different samples were displayed.

LC/MS non-targeted metabolome analysis

Metabonomic analysis of mouse intestinal contents were carried on with Dionex U3000 UHPLC (Thermo Fisher Scientific) ultra-high performance liquid phase tandem QE plus (Thermo Fisher Scientific) high-resolution mass spectrometer composed of liquid-mass spectrometry system. It was conducted by OE Biotech Company (Shanghai, China). The raw data was processed by the metabolomics processing software Progenesis QI v2.3 (Nonlinear Dynamics, Newcastle, UK) for baseline filtering, peak identification, integration, retention time correction, peak alignment and normalization. For the extracted data, the ion peaks with missing values (0 value)> 50% in the group were deleted, and the 0 value with half of the minimum value was replaced. The compound was scored according to the compound qualitative results (Score), and then the compound was qualitatively obtained for screening, and the screening standard was 40 points (full score is 60 points), and the qualitative results were deemed inaccurate and deleted if the score was less than 40 points. Finally, the positive and negative ion data was combined into a data matrix table, which contained all the information extracted from the original data that could be used for analysis, and subsequent analysis was based on this including multivariate statistical analysis, univariate statistical analysis, differential metabolite screening and metabolic pathway enrichment analysis.

QUANTIFICATION AND STATISTICAL ANALYSIS

Data are presented as mean ± standard error of the mean (SEM). All data were analyzed using GraphPad Prism 6.01 (GraphPad Software, USA). The data were analyzed for normal distribution before performing statistical analysis. In microbiota analysis, the differences between the two groups were statistically analyzed by Wilcoxon Rank-Sum test, and the differences between the other two groups were statistically analyzed by two-way unpaired Student's t test. A $p < 0.05$ was considered as statistical difference. Statistical parameters are shown with p value: *: $p < 0.05$, **: $p < 0.01$, ***: $p < 0.001$, ****: $p < 0.0001$.